Available online at www.sciencedirect.com

ScienceDirect

Transportation Research Procedia 2 (2014) 724 – 732

Transportation Research Procedia

www.elsevier.com/locate/procedia

The Conference on Pedestrian and Evacuation Dynamics 2014 (PED2014)

Validating social force based models with comprehensive real world motion data

Stefan Seer [a,*], Christian Rudloff [a], Thomas Matyus [a], Norbert Brändle [a]

[a]*AIT Austrian Institute of Technology, Mobility Department, Giefinggasse 2, Vienna, 1210, Austria*

Abstract

Over the last years multiple variations of the Social Force model have been proposed. While most of the available force-based models are calibrated on observed human movement data, validation for investigating the model characteristics, e.g. variance in parameter values, is still sparse. We present a novel methodology for validating Social Force based models which investigates the reproducibility of human movement behavior on the individual trajectory level with real-world movement data. Our approach estimates model parameter values and their distribution with non-linear regression on observed trajectory data, where the resulting variances of the parameter values represent the model's validity. We demonstrate our approach on a comprehensive (235 pedestrians) and highly accurate (within a few centimeters) set of human movement trajectories obtained from real-world pedestrian traffic with bidirectional flow using an automatic people tracking approach based on Kinect sensors. We validate the Social Force model of Helbing and Molnár (1995), Helbing and Johansson (2009) and Rudloff et al. (2011).

Peer-review under responsibility of Department of Transport & Planning Faculty of Civil Engineering and Geosciences Delft University of Technology

Keywords: crowd dynamics; model validation; parameter estimation; non-linear regression; social force model; real-world data

1. Introduction

Nowadays, pedestrian simulation is used in many different applications and has proven to be a valuable tool to support the design and evaluation of architectural plans, to estimate traffic needs and capacities, to increase safety, efficiency and comfort in crowded areas and to analyze different scenarios for emergency evacuations. Microscopic models, in particular, allow to simulate very detailed human movement interactions on the individual level and thus can reveal a multitude of useful information for designers and planners of infrastructures and urban places. As computational power increases, and becomes more affordable, these microscopic models are also more frequently used for highly complex environments which comprise crowd flows of several 10,000 individuals such as airports, public transit hubs and mass events.

Human movement involves different behavioral processes which according to Hoogendoorn and Bovy (2004) can be roughly grouped into a *strategic* (choice of general behavior, e.g. destinations, and activity area), a *tactical* (activity scheduling and route choice) and an *operational* (short range behavior and instantaneous decisions) level. This paper

* Corresponding author. Tel.: +43(0) 50550-6478 ; fax: +43(0) 50550-6439.
E-mail address: stefan.seer@ait.ac.at

Peer-review under responsibility of Department of Transport & Planning Faculty of Civil Engineering and Geosciences Delft University of Technology
doi:10.1016/j.trpro.2014.09.080

focuses on the microscopic modeling of pedestrian movement on the operational level where a model generally has to take care of the following two tasks: 1) each pedestrian wants to walk with an individual desired speed while 2) keeps a certain distance from other pedestrians and static obstacles.

Various academic tools, e.g. NOMAD (Hoogendoorn (2003)), Hermes (Holl et al. (2014)), and commercial software, e.g. SimWalk (Savannah Simulations), PedGo (TraffGo), VisWalk (PTV), MassMotion (Oasys Software), Cast (ARC), exist. On the operational level, many of them are based or are closely related to the Social Force approach which was first described in Helbing and Molnár (1995). Inspired by the principles of the Social Force model different variations have been proposed in the scientific literature such as in Lakoba et al. (2005), Parisi et al. (2009), Seyfried et al. (2006).

In order to develop a model that is able to represent realistic movement behavior one has to perform model calibration and a validation of the results. Therefore, observations of real pedestrians are needed which can be obtained from (controlled) experiments (Daamen and Hoogendoorn (2012)) or from real-world measurements. Quantitative data from human movement observations can comprise, for instance, travel times, flow rates, speed-density fundamental relation or even trajectories of individual pedestrians. The process of collecting individual trajectories to calibrate microscopic models is cumbersome since robust (including all individuals being in a scene at the same time), accurate (within a few centimeters) and comprehensive (minimum of several 100 individuals) trajectories from various scenarios (e.g. different pedestrian densities) are needed. To meet these high standards, typically video footage of pedestrian movement is recorded and annotated either manually or semi-automatically (Boltes et al. (2010)). Recently, an approach using the Microsoft Kinect as a low cost sensor for obtaining highly accurate people trajectories (Seer et al. (2012)) was shown to be a valuable tool for developers of microscopic models in the calibration and validation process. In this paper we also rely on the data set collected in the work of Seer et al. (2012).

Several calibration procedures were suggested in the literature where in particular two distinct approaches are predominant: the first is model estimation by maximum likelihood or nonlinear least square methods (e.g. Hoogendoorn et al. (2007) or Ko et al. (2013)). However, as shown in Rudloff et al. (2014) this approach suffers strongly from errors in variables due to the large measurement errors from data collection using pure video data. The second approach involves the comparison of real and simulated trajectories (e.g. Moussaïd et al. (2009), Rudloff et al. (2011)) and hence is time consuming as a complete simulation run is needed during each optimization step.

Since the quality of the trajectories from Seer et al. (2012) is significantly higher compared with those automatically extracted from video footage, it needs to be determined if the added data quality makes a nonlinear least square estimation feasible. Many of the available force-based models are calibrated on observed human movement data (e.g. Campanella et al. (2014)) However, validation for investigating the model characteristics, e.g. variance in parameter values, is still sparse. It needs to be determined if the estimated parameters can explain the diverse behavior of pedestrians or if parameters need to be more flexible and differ for different pedestrians. This would suggest that a Social Force model with a single parameter set might not be able to explain pedestrian behavior in different situations for example with respect to different densities.

The contribution of this work is to present a methodology for validating Social Force based models which investigates the reproducibility of human movement behavior on the individual trajectory level for different settings with real-world movement data. Our approach estimates model parameter values and their distribution with non-linear regression on observed trajectory data, where the resulting variances of the parameter values represent the model's validity. We demonstrate our approach on a comprehensive (235 pedestrians) and highly accurate (within a few centimeters) set of human movement trajectories obtained from real-world pedestrian traffic with bidirectional flow using an automatic people tracking approach based on Kinect sensors (Seer et al. (2012)). We validate the Social Force model of Helbing and Molnár (1995), Helbing and Johansson (2009) and Rudloff et al. (2011).

The remainder of this paper is structured as follows. Section 2 describes the variants of the Social Force model that are used in this work. In Section 3, we describe the data set originating from real-world observations and the preprocessing of the trajectories. Section 4 presents our methods of model calibration and validation also including the results. Section 5 concludes the main findings and discusses future research directions.

2. Variants of the Social Force model

In the scientific literature, different variants of the Social Force approach have been described. All of them are based on the principle of modeling behavioral changes guided by so-called *social forces*. Given that the movement of

a person depends on velocity and hence on acceleration, the principle of the Social Force model aims at representing individual walking behavior as a sum of different accelerations as

$$\mathbf{f}_\alpha(t) = \frac{v_\alpha^0 \mathbf{e}_\alpha - \mathbf{v}_\alpha}{\tau_\alpha} + \sum_{\beta \neq \alpha} \mathbf{f}_{\alpha\beta}(t) + \sum_i \mathbf{f}_{\alpha i}(t) \tag{1}$$

The acceleration $\mathbf{f}_\alpha$ at time t of an individual α towards a certain goal is defined by the desired direction of movement $\mathbf{e}_\alpha$ with a desired speed v_α^0. Here, the current velocity $\mathbf{v}_\alpha$ is adapted to the desired speed v_α^0 within a certain relaxation time τ_α. The movement of a pedestrian α is influenced by other pedestrians β, which is modeled as a repulsive acceleration $\mathbf{f}_{\alpha\beta}$. A similar repulsive behavior for static obstacles i (e.g. walls) is represented by the acceleration $\mathbf{f}_{\alpha i}$. For notational simplicity, we omit the dependence on time t for the rest of this section.

From the set of different formulations of the Social Force model available in the scientific literature, we compare three variations of the Social Force model based on the general formulation (1).

Model A: The first model from Helbing and Molnár (1995) is based on a circular specification of the repulsive force given as

$$\mathbf{f}_{\alpha\beta}^A = A_\alpha e^{-\frac{\left(r_\alpha + r_\beta - \left\|\mathbf{d}_{\alpha\beta}\right\|\right)}{B_\alpha}} \cdot \frac{\mathbf{d}_{\alpha\beta}}{\left\|\mathbf{d}_{\alpha\beta}\right\|} \tag{2}$$

where r_α and r_β denote the radii of pedestrians α and β, and $\mathbf{d}_{\alpha\beta}$ is the distance vector pointing from pedestrian α to β. The interaction of pedestrian α is parameterized by the strength A_α and the range B_α, where their values are determined in the model calibration process.

Model B: The second model uses the elliptical specification of the repulsive force as described in Helbing and Johansson (2009) determined by

$$\mathbf{f}_{\alpha\beta}^B = A_\alpha e^{-\frac{w_{\alpha\beta}}{B_\alpha}} \cdot \frac{\left\|\mathbf{d}_{\alpha\beta}\right\| + \left\|\mathbf{d}_{\alpha\beta} - \mathbf{y}_{\alpha\beta}\right\|}{2w_{\alpha\beta}} \cdot \frac{1}{2}\left(\frac{\mathbf{d}_{\alpha\beta}}{\left\|\mathbf{d}_{\alpha\beta}\right\|} + \frac{\mathbf{d}_{\alpha\beta} - \mathbf{y}_{\alpha\beta}}{\left\|\mathbf{d}_{\alpha\beta} - \mathbf{y}_{\alpha\beta}\right\|}\right) \tag{3}$$

where the semi-minor axis $w_{\alpha\beta}$ of the elliptic formulation is given by

$$w_{\alpha\beta} = \frac{1}{2}\sqrt{\left(\left\|\mathbf{d}_{\alpha\beta}\right\| + \left\|\mathbf{d}_{\alpha\beta} - \mathbf{y}_{\alpha\beta}\right\|\right)^2 - \left\|\mathbf{y}_{\alpha\beta}\right\|^2} \tag{4}$$

with $\mathbf{y}_{\alpha\beta} = (\mathbf{v}_\beta - \mathbf{v}_\alpha)\Delta t$. Here, the velocity vectors $\mathbf{v}_\alpha$ and $\mathbf{v}_\beta$ of pedestrians α and β are included allowing to take into account the step size of pedestrians.

Model C: The third model is an implementation of Rudloff et al. (2011) in which the repulsive force is split into one force directed in the opposite of the walking direction, i.e. the *deceleration force*, and another one perpendicular to it, i.e. the *evasive force*. Here, the repulsive force is given as

$$\mathbf{f}_{\alpha\beta}^C = \mathbf{n}_\alpha \underbrace{A_n e^{\frac{-B_n \phi_{\alpha\beta}^2}{v_{\text{rel}}} - C_n \left\|\mathbf{d}_{\alpha\beta}\right\|}}_{\text{deceleration force}} + \mathbf{p}_\alpha \underbrace{A_p e^{\frac{-B_p \left|\phi_{\alpha\beta}\right|}{v_{\text{rel}}} - C_p \left\|\mathbf{d}_{\alpha\beta}\right\|}}_{\text{evasive force}} \tag{5}$$

where $\mathbf{n}_\alpha$ is the direction of movement of pedestrian α and $\mathbf{p}_\alpha$ its perpendicular vector directing away from pedestrian β. Furthermore, $\phi_{\alpha\beta}$ is the angle between $\mathbf{n}_\alpha$ and $\mathbf{d}_{\alpha\beta}$ and v_{rel} denotes the relative velocity between pedestrians α and β. Model parameters are denoted by A_n, B_n, C_n, A_p, B_p and C_p.

The repulsive force from static obstacles $\mathbf{f}_{\alpha i}$ is modeled by using the functional form as given by the repulsive force for pedestrians from Model B in all cases. Here, the point of an obstacle i closest to pedestrian α replaces the position β and $\mathbf{v}_i$ is set to zero. Furthermore, we take into account that pedestrians have a higher response to other pedestrians in front of them by including an anisotropic behavior, as described in Helbing and Johansson (2009), into the first two formulations.

3. Measures for human movement

The data used in this paper for model calibration and validation originates from a real-world setting at the Massachusetts Institute of Technology (MIT)'s Infinite Corridor as described in Seer et al. (2012). This hallway serves as the most direct indoor route between the east and west ends of the campus and is highly frequented by students and visitors. In order to collect a large dataset on pedestrian movement, three Kinect sensors were suspended from the ceiling and covered a total scanning area of roughly 2 m x 6 m. By applying the automatic tracking approach from Seer et al. (2012), we obtain a set

$$\mathcal{T}' = \left\{ [t'_\alpha \; x'_\alpha \; y'_\alpha]^T \right\}_{\alpha \in N,} \tag{6}$$

of human trajectories represented by $3 \times D'_\alpha$ matrices where N is the set of pedestrians, D'_α is the number of positions in the trajectory of a pedestrian α and the matrices are composed of a vector of timestamps t'_α and 2D positions $\mathbf{x}'_\alpha = [x'_\alpha \; y'_\alpha]^T$. As a result of the automated tracking, each trajectory in $\mathcal{T}'$ consists of coordinate sequences of arbitrary length and time. To have trajectory data points at a regular time interval $\Delta t = 0.1$ seconds and to remove small local variations along trajectories, each trajectory in $\mathcal{T}'$ was resampled. Hence, we obtained a set of resampled trajectories $\mathcal{T}$ with $t_\alpha = \left[t^{in}_\alpha, t^{in}_\alpha + \Delta t, t^{in}_\alpha + 2\Delta t, \ldots, t^{out}_\alpha \right]$, $t^{in}_\alpha = \left\lfloor t'_{\alpha 1} / \Delta t \right\rfloor \Delta t$ and $t^{out}_\alpha = \left\lfloor t'_{\alpha D'_\alpha} / \Delta t \right\rfloor \Delta t$. The corresponding x_α and y_α at regular time intervals t_α are obtained by cubic spline approximation (see de Boor (2001)) with a smoothing parameter $p = 0.98$.

Fig. 1a illustrates the automatically obtained trajectories from a walking experiment with a single centralized obstacle in the scene. This walking experiment was performed under real world conditions, meaning that the individuals traversing MIT's Infinite Corridor had no information about being observed. The red and blue trajectories in Fig. 1a represent the two walking lanes in opposite directions which people form most of the time. Fig. 1b shows the trajectory density map using a kernel density estimation with a normal kernel function and a bandwidth of 0.1 m. This reveals the main paths located on both sides of the corridor which pedestrians use to evade from the centralized obstacle.

From the trajectories one can directly extract the acceleration $\tilde{\mathbf{f}}_\alpha(t)$ for each individual α at each time instance t from the collected trajectories according to

$$\tilde{\mathbf{f}}_\alpha(t) := \left[\tilde{f}^x_\alpha(t), \tilde{f}^y_\alpha(t) \right] = \left[\frac{(x_\alpha(t+1) - x_\alpha(t)) - (x_\alpha(t) - x_\alpha(t-1))}{\Delta t^2}, \frac{(y_\alpha(t+1) - y_\alpha(t)) - (y_\alpha(t) - y_\alpha(t-1))}{\Delta t^2} \right] \tag{7}$$

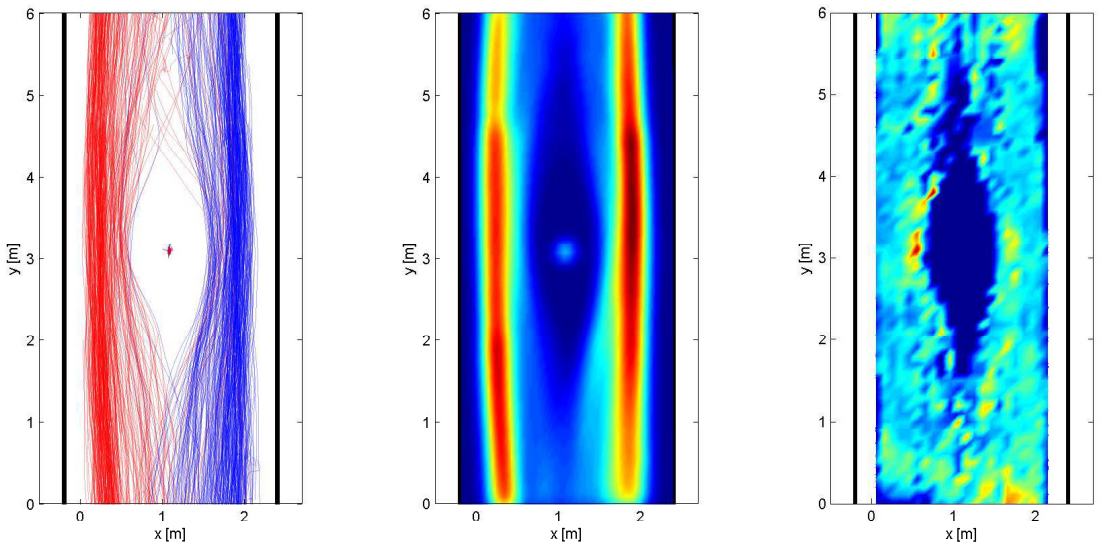

(a) (b) (c)

Fig. 1. Observed (a) trajectories with walking directions encoded in red and blue, (b) density map and (c) acceleration map based on real-world observations in a corridor with a single centralized obstacle.

Fig. 1c shows the time averaged accelerations inside the scanning area. As expected the accelerations are higher the nearer pedestrians pass the central obstacle. Besides, in the lower right and in the upper left part of the figure, the areas where people start to deviate can be identified. We derive the position and the desired goal for a pedestrian α from the first point at time t_α^{in} and the last point at t_α^{out} of the associated observed trajectory $\mathcal{T}_\alpha$. The desired velocity v_α^0 of pedestrian α is defined as the 95th percentile of the observed velocities. The magnitude of the current velocity vector $\mathbf{v}_\alpha$ is set equal to v_α^0, and it directs towards the pedestrian's desired goal. Furthermore, we set for each simulated pedestrian $r = 0.25$ and $\tau = 0.5$.

Since only a section of the corridor was observed, it has to be guaranteed that all individuals influencing each other's movements (i.e. persons closer than 2 m in front or 1 m behind) are present in the scene. We selected a subset of trajectories $\mathcal{T}^S$ corresponding to a set of pedestrians M, where M is a subset of N, that fulfills two constraints: 1) they are long enough, i.e. start below $y = 1$ m and end above $y = 4$ m and vice versa without stops, and 2) all other individuals who are present or appear during the time span of the relevant trajectory have to be present for the whole time span or until they leave the scene. For the subsequent calibration, we only use segments of trajectories in $\mathcal{T}^S$, which in upward direction are between $y = 1$ m and $y = 4$ m and between $y = 5$ m and $y = 2$ m for the downward direction (see Fig. 1). Hence, we denote the start and end time of the segments by t_α^{start} and t_α^{end}.

4. Model estimation and validation results

As a first step, we examine the validity of estimating the parameters of the investigated Social Force models using non-linear least square estimation. In the estimation procedure we use the objective function

$$f_{obj}(\theta) = \sum_{\alpha \in M} \sum_{t=t_\alpha^{start}}^{t_\alpha^{end}} \left(\left(\tilde{f}_\alpha^x(t) - f_\alpha^x(t,\theta) \right)^2 + \left(\tilde{f}_\alpha^y(t) - f_\alpha^y(t,\theta) \right)^2 \right) \tag{8}$$

where $\mathbf{f}_\alpha(t,\theta) = \left[f_\alpha^x(t,\theta), f_\alpha^y(t,\theta) \right]$ is the acceleration at time t given a parameter set θ. The optimization uses the gradient based method `fmincon` in MATLAB. This method also allows to extract the Hessian matrix H_f of f_{obj} at the estimated optimal parameter set $\hat{\theta}$, which in turn gives an estimate of the covariance matrix of the parameters as $Cov(\hat{\theta}) = H_f^{-1}$. Using $f_{obj}(\theta)$ the three Social Force models are calibrated in two ways: by estimating the parameters for all pedestrians at once (*general calibration*) and by estimating them for the first 33 pedestrians (*personalized calibration*) in order to examine if the models transfer well to single pedestrians. The results of the parameter estimation for all three models can be seen in Table 1.

Table 1. Estimated parameter values for the three models with standard deviations of the parameters in brackets. Parameters significantly different from zero are in bold letters.

Model	Value of f_{obj} General Calibration	Avg. value of f_{obj} and (std) Personalized Calibration	Parameter	Parameter Value and (std) General Calibration	Avg. Parameter Value and (std) Personalized Calibration
Model A	2189.4	7.0374 (5.1200)	A	**0.1634** (0.0104)	0.4500 (04050)
			B	**4.1554** (0.6535)	13.4651 (18.3852)
			A_w	1.9534 (1.2244)	8.8260 (15.4703)
			B_w	**0.1090** (0.0231)	0.2882 (07676)
Model B	2244.4	7.9460 (5.7311)	A	**0.1845** (0.0205)	0.4213 (0.3941)
			B	**5.9334** (1.6812)	5.7032 (0.7336)
			A_w	**1.9534** (0.6035)	1.5540 (2.1782)
			B_w	**0.1366** (0.0248)	0.7415 (2.7448)
Model C	1925.2	6.1492, (3.8987)	A_n	**0.2615** (0.0551)	1.0310(1.9060)
			B_n	**0.4026** (0.1238)	2.0385 (5.2833)
			C_n	**2.1614** (0.3728)	2.3522 (0.9944)
			A_p	**1.5375** (0.3084)	1.8980 (0.8775)
			B_p	**0.4938** (0.1041)	0.9656 (0.9226)
			C_p	**0.5710** (0.1409)	0.9190 (0.8823)
			A_w	**0.3280** (0.1481)	0.7450 (1.5747)
			B_w	**0.1871** (0.0563)	1.8044 (4.1646)

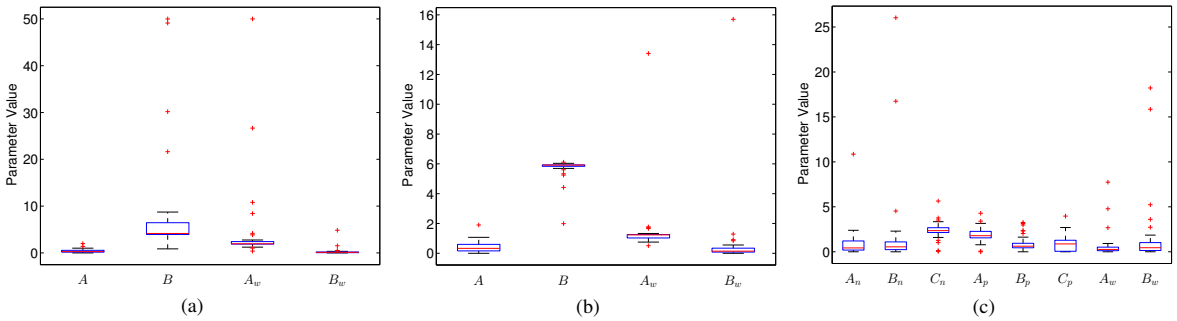

Fig. 2. Boxplots with estimated parameter values from personalized calibration for (a) Model A, (b) Model B and (c) Model C.

The results show that the objective function is best for Model C and that Model A with the original circular formulation outperforms Model B with the elliptical form. Despite the large number of data points (7799 from 235 trajectories) the parameters estimated in the general calibration are not all significant, which suggests either that the information contained in the data is not sufficient or that there is a strong variation in behavior between different pedestrians. It can be seen from Table 1 that the parameters of the personalized calibration are higher on average than the parameters of the general calibration and their standard deviations are rather large. Fig. 2 shows that all these parameters lie in a relatively small band and that there are only a few outliers. This, together with the plots in Fig. 3, suggest that some pedestrians react much stronger than others to obstacles. Furthermore, the accelerations from the parameter set estimated by the general calibration do not suffice to model this strong reaction.

In order to test if the results from the non-linear least square estimation in a model reproduce good reaction to other pedestrians, it is important to investigate the collision avoidance behavior of the model. As an example, we show in Fig. 4 the accelerations in x and y directions resulting from the three models with parameters from general calibration. In this setting a pedestrian is walking with a velocity of $[0, 1]$ towards a goal upwards in y-direction while another pedestrian stands at position $[1.1, 3]$. The accelerations resulting from the model are calculated for all positions in a 2D regular grid with grid size 0.1 m. One can see that all models show collision avoidance behavior. Due to model restrictions Models A and B do not show much acceleration to the side when a pedestrian is walking towards an obstacle straight ahead, but rather just decelerates the pedestrian. In comparison Model C does show avoidance behavior in that case. Overall, the models show a promising behavior, however, a calibration should be performed on denser scenarios to ensure that the collision avoidance works in those cases as well.

It was noted in Rudloff et al. (2014) that Social Force models have relatively large parameter areas where they behave very similarly with respect to closeness of trajectories. However, the validation results in Fig. 3 show that the different parameter sets from personalized calibration (see Fig. 2) produce significant variations in the behavior of accelerations in x and y-directions. In particular there are some outliers in the acceleration behavior which result from the fact that for some pedestrians the parameters from personalized calibration are much larger than for the general calibration using the points from all trajectories.

5. Conclusion

We presented a procedure to estimate model parameter values for the validation of Social Force based approaches using real-world pedestrian motion data. By using a comprehensive and highly accurate set of human movement trajectories we were able to evaluate the model parameter values and their distribution of three different Social Force variants based on non-linear least square parameter estimation. Due to the high quality of the trajectory data used in this work, the problem of errors in variables in the calibration is reduced. This leads to parameter values for the investigated models which reveal good collision avoidance behavior, despite the relatively simple scenario with low pedestrian densities. Hence, the parameter values in this paper have to be taken with caution. A recalibration with denser scenes should be performed to ensure that average pedestrian behavior can be reproduced well. This would be in accordance with previous results (e.g. Johansson et al. (2007)) where the Social Force model proved to be able to reproduce macroscopic characteristics, such as flow-density relations, well.

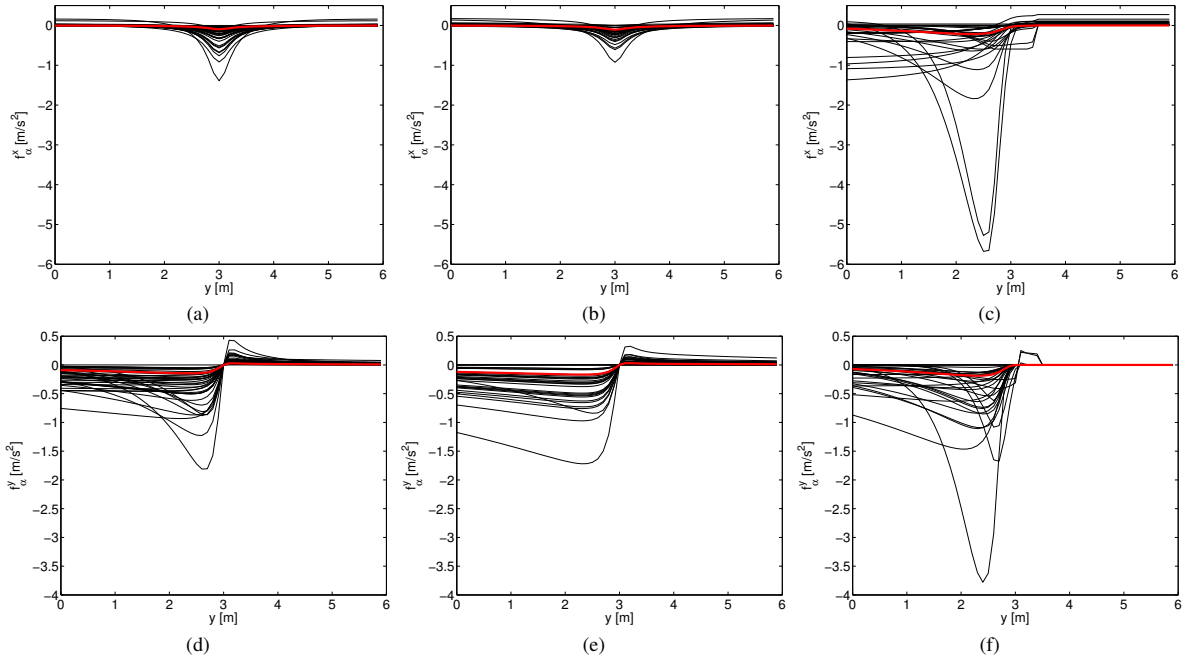

Fig. 3. Accelerations calculated with Model A (left), B (middle) and C (right) in x-direction (a, b and c) and y-direction (d, e and f) for parameters from personalized (black lines) and general calibration (bold red line).

It has to be noted though that parameters estimated for each pedestrian separately show large standard deviations. The primary reason are large deviations of the parameter values of a few pedestrians. This suggests that the trajectories of those pedestrians include large evasive maneuvers that cannot be described by the model using the parameter set with the general calibration.

The results of our validation weakens the claim that the Social Force model as a microscopic model can reproduce human behavior at a trajectory level for each single pedestrian. While it performs well for the majority of pedestrians, the behavior of single pedestrians with more unusual or erratic behavior might not be well predicted using Social Force approaches. However, pedestrians with unusual behavior might be important for the overall behavior of the crowd, since other pedestrians need to react to them. This reveals the need for future discussion on how to calibrate Social Force models and how to interpret the simulation results of these models. Even in simple scenarios, such as the one presented in this work, the investigated models cannot be expected to reproduce all trajectories exactly.

It also needs to be discussed if the calibration of Social Force models on pedestrian trajectories is a good approach since the outliers in behavior might strongly influence the parameters. Other objective functions involving macroscopic measures like densities and travel times might produce more reliable models for the prediction of these important features. This approach needs to be evaluated in future. Furthermore, we suggest that all other microscopic pedestrian simulation models should be investigated with respect to these considerations.

Acknowledgements

This work has been supported by the Austrian Ministry for Traffic, Innovation, and Technology (BMVIT). The data used in this work was collected as part of a collaboration with the MIT Senseable City Lab. The authors would like to thank Carlo Ratti and David Lee for their valuable support in conducting this research.

References

Boltes, M., Seyfried, A., Steffen, B., Schadschneider, A., 2010. Automatic Extraction of Pedestrian Trajectories from Video Recordings, in: Klingsch, W.W.F., Rogsch, C., Schadschneider, A., Schreckenberg, M. (Eds.), Proceedings of the Conference on Pedestrian and Evacuation

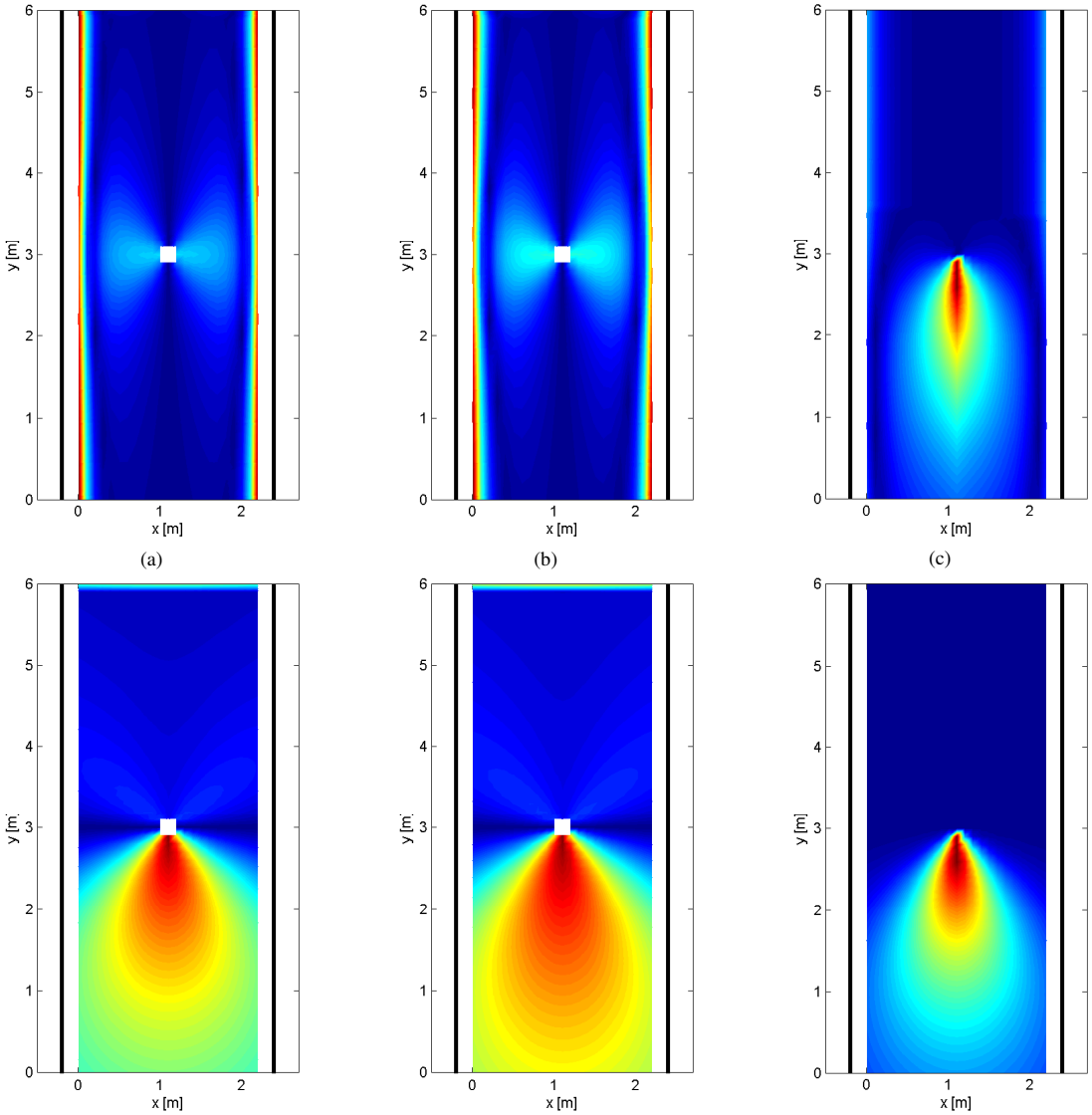

Fig. 4. Accelerations in x-direction (a, b and c) and y-direction (d, e and f) calculated using Model A (left), B (middle) and C (right) with parameters from general calibration.

Dynamics (PED 2008), Springer, Berlin, Heidelberg. pp. 43–54. URL: http://www.springerlink.com/index/n420218717p18252.pdf.

Campanella, M., Hoogendoorn, S., Daamen, W., 2014. Quantitative and Qualitative Validation Procedure for General Use of Pedestrian Models, in: Weidmann, U., Kirsch, U., Schreckenberg, M. (Eds.), Proceedings of the Conference on Pedestrian and Evacuation Dynamics 2012 (PED2012), Springer International Publishing. pp. 891–905.

Daamen, W., Hoogendoorn, S.P., 2012. Calibration of Pedestrian Simulation Model for Emergency Doors for Different Pedestrian Types, in: Proceedings of the Transportation Research Board 91st Annual Meeting (TRB 2012), Washington D. C., USA.

de Boor, C., 2001. A Practical Guide to Splines. second ed., Springer-Verlag, New York.

Helbing, D., Johansson, A., 2009. Pedestrian, Crowd and Evacuation Dynamics. Encyclopedia of Complexity and Systems Science 16, 6476–6495.

Helbing, D., Molnár, P., 1995. Social Force Model for Pedestrian Dynamics. Physical Review E 51, 4282–4286. URL: http://link.aps.org/doi/10.1103/PhysRevE.51.4282, doi:10.1103/PhysRevE.51.4282.

Holl, S., Schadschneider, A., Seyfried, A., 2014. Hermes: An Evacuation Assistant for Large Arenas, in: Weidmann, U., Kirsch, U., Schreckenberg,

M. (Eds.), Pedestrian and Evacuation Dynamics 2012, Springer International Publishing. pp. 345–349.

Hoogendoorn, S., Daamen, W., Landman, R., 2007. Microscopic Calibration and Validation of Pedestrian Models Cross-Comparison of Models using Experimental Data, in: Waldau, N., Gattermann, P., Knoflacher, H., Schreckenberg, M. (Eds.), Pedestrian and Evacuation Dynamics 2005 (PED2005), Springer Berlin Heidelberg. pp. 253–265.

Hoogendoorn, S.P., 2003. Microscopic Simulation of Pedestrian Flows, in: Proceedings of the Transportation Research Board 82nd Annual Meeting (TRB 2003), Washington D. C., USA.

Hoogendoorn, S.P., Bovy, P.H.L., 2004. Pedestrian Route-Choice and Activity Scheduling Theory and Models. Transportation Research Part B: Methodological 38, 169–190. URL: http://ideas.repec.org/a/eee/transb/v38y2004i2p169-190.html.

Johansson, A., Helbing, D., Shukla, P.K., 2007. Specification of the Social Force Pedestrian Model by Evolutionary Adjustment to Video Tracking Data. Advances in Complex Systems 10, 271–288.

Ko, M., Kim, T., Sohn, K., 2013. Calibrating a Social-Force-Based Pedestrian Walking Model based on Maximum Likelihood Estimation. Transportation 40, 91–107.

Lakoba, T.I., Kaup, D.J., Finkelstein, N.M., 2005. Modifications of the Helbing-Molnar-Farkas-Vicsek Social Force Model for Pedestrian Evolution. Simulation 81, 339–352.

Moussaïd, M., Helbing, D., Garnier, S., Johansson, A., Combe, M., Theraulaz, G., 2009. Experimental study of the behavioural mechanisms underlying self-organization in human crowds. Proceedings of the Royal Society - Biological Sciences 276, 2755–2762. URL: http://rspb.royalsocietypublishing.org/cgi/doi/10.1098/rspb.2009.0405, doi:10.1098/rspb.2009.0405.

Parisi, D.R., Gilman, M., Moldovan, H., 2009. A Modification of the Social Force Model can Reproduce Experimental Data of Pedestrian Flows in Normal Conditions. Physica A: Statistical Mechanics and its Applications 388, 3600–3608.

Rudloff, C., Matyus, T., Seer, S., 2014. Comparison of Different Calibration Techniques on Simulated Data, in: Weidmann, U., Kirsch, U., Schreckenberg, M. (Eds.), Pedestrian and Evacuation Dynamics 2012 (PED2012). Springer International Publishing, pp. 657–672.

Rudloff, C., Matyus, T., Seer, S., Bauer, D., 2011. Can Walking Behavior be Predicted? An Analysis of the Calibration and Fit of Pedestrian Models. Transportation Research Record 2264.

Seer, S., Brändle, N., Ratti, C., 2012. Kinects and Human Kinetics: A New Approach for Studying Crowd Behavior. Submitted to: Transportation Research Part C: Emerging Technologies URL: http://arxiv.org/abs/1210.2838.

Seyfried, A., Steffen, B., Lippert, T., 2006. Basics of Modelling the Pedestrian Flow. Physica A: Statistical Mechanics and its Applications 368, 232–238.